IEEE Access
Multidisciplinary : Rapid Review : Open Access Journal

Received February 5, 2021, accepted March 5, 2021, date of publication March 9, 2021, date of current version March 18, 2021.

Digital Object Identifier 10.1109/ACCESS.2021.3065008

Disturbance Decoupling and Tracking Controller Design for Lateral Vehicle Dynamics

MOHAMMAD REZA SATOURI[1], ABOLHASSAN RAZMINIA[1], SALEH MOBAYEN[2,3], AND PAWEŁ SKRUCH[4], (Senior Member, IEEE)

[1]Dynamical Systems and Control (DSC) Research Laboratory, Department of Electrical Engineering, School of Engineering, Persian Gulf University, Bushehr 7516913817, Iran
[2]Department of Electrical Engineering, University of Zanjan, Zanjan 45371-38791, Iran
[3]Future Technology Research Center, National Yunlin University of Science and Technology, Yunlin 64002, Taiwan
[4]Department of Automatic Control and Robotics, AGH University of Science and Technology, 30-059 Kraków, Poland

Corresponding authors: Abolhassan Rzaminia (razminia@pgu.ac.ir) and Saleh Mobayen (mobayens@yuntech.edu.tw)

This work was supported in part by the Ministry of Science and Technology (MOST), Taiwan, under Grant MOST 110-2222-E-224-001-, and in part by the Faculty of Electrical Engineering, Automatics, Computer Science and Biomedical Engineering of the AGH University of Science and Technology, Cracow, Poland under research subsidy no. 16.16.120.773.

ABSTRACT This paper addresses an augmented nonlinear lateral vehicle and lane keeping dynamics in the presence of some unknown disturbances. In a geometric basin, considering unobservable spaces, their orthogonal complements, and using control invariant properties, a disturbance decoupling mechanism is designed for the mentioned dynamics. Afterward, a nonlinear tracking controller is designed to steer the vehicle on a reference path. The obtained disturbance decoupling and tracking controllers are implemented on a typical passenger car in a simulation environment to demonstrate the effectiveness and performance of the proposed method. It is shown that the controller decouples both the uniformly distributed and exponentially attenuated disturbances from the output.

INDEX TERMS Control invariant, disturbance decoupling, exponential stability, nonlinear lateral vehicle dynamics, tracking control.

I. INTRODUCTION

Autonomous vehicle as a progressing technology has now attracted many attentions from various different disciplines and as a result, most giant auto manufacturers like BMW and Toyota are investing billions of dollars for developing this technology. Thanks to advances in electronics and telecommunication systems, the technology of such vehicles has a great growth. However, many challenges still remain in this ongoing area [1]. Some of these challenges can be classified in the following categories: lane change control [2], model recognition [3], stability control [4], and tracking control [5], [6].

The appearance of the control system can be seen in different levels of dynamics of vehicle. Vehicle yaw, lateral and longitudinal dynamics control are discussed in literatures with various control methods like sliding mode [7]–[9], output feedback [10], [11], fuzzy methods [12], [13], model predictive control [13], [14], gain scheduling [15], [16], linear quadratic regulator [17] and neural networks [18]. Among these diverse control systems, disturbance decoupling is one of the most important topics in which, in the presence of some unwanted conditions, the vehicle has to be comforted for its passenger or track a desired trajectory.

For confronting with disturbances, several methods are developed in control systems where a popular one is a robust control technique [19]–[21]. In this method, different approaches like gain scheduling [22] and fuzzy technique [23] are employed. There is another method to deal with disturbances which decouples them from desired outputs, called disturbance decoupling technique. Although disturbance decoupling is widely used in engineering applications like [24]–[30], there is a few research about applications of this technique in autonomous vehicles [31]. A powerful approach for disturbance decoupling is a geometric one, which in spite of its advantages, like giving sense to control designers, is not considered in the researches of autonomous vehicles yet.

In this paper, at the first step, a general nonlinear lateral dynamics of an autonomous vehicle is derived. Afterward, using some simplifying assumptions, the nonlinearity of the obtained model is reduced and hence the model is augmented with the lane keeping dynamics. Then, the error dynamics are calculated by subtracting the reference dynamics from the overall ones. All classes of disturbances that are decouplable from lateral deviation are investigated via a geometric

The associate editor coordinating the review of this manuscript and approving it for publication was Hai Wang.

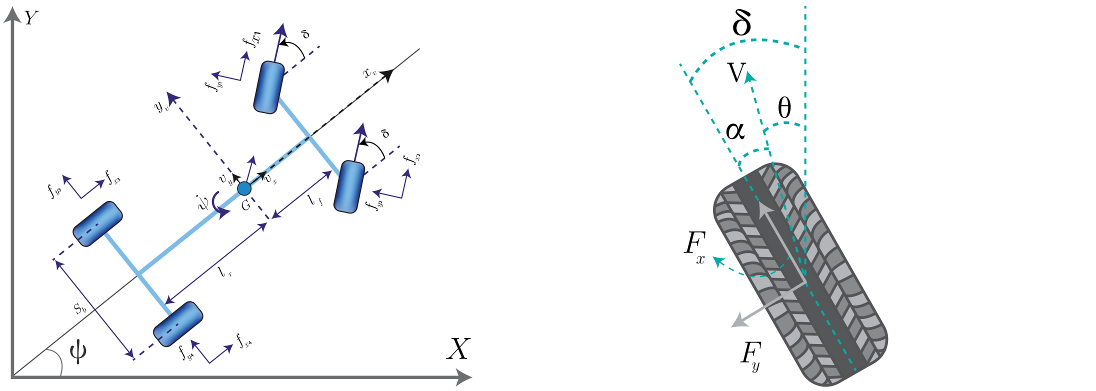

(a) Vehicle's parameters. (b) Tire side slip angles.

FIGURE 1. **Vehicle's parameters and tire side slip angles.**

approach. Using control invariant property, a disturbance decoupling controller is designed and then, a tracking controller is proffered which makes the states exponentially track their references in the absence of the disturbances. In the presence of the disturbances, the error dynamics remain stable and just the lateral deviation, which is decoupled from the disturbances, exponentially converges to zero. Finally, The disturbance decoupling and tracking controller, and the obtained results are summarized in a theorem. To show the effectiveness of the proposed controller, we implement the technique on a typical vehicle in the presence of two kinds of disturbances: exponentially attenuated disturbances and uniformly distributed ones. Our main contributions can be summarized as follows:

1) Using a geometric approach for disturbance decoupling purpose in the autonomous vehicles for the first time.
2) Utilizing nonlinear dynamics of the lateral vehicle's motion which reduces the errors arise from linearization.
3) Validating the robustness of the proposed algorithm with respect to vehicle parameter uncertainties.

The organization of the paper is as follows: Section II discusses the lateral vehicle dynamics augmented with lane keeping ones and states what the problem is. The disturbance decoupling and tracking controllers are investigated in Section III. Some illustrative examples are employed to verify the importance of the achieved results which brought in Section IV. Finally, some concluding remarks are presented in Section V.

II. MODEL DESCRIPTION AND PROBLEM STATEMENT

As a general description of our problem, at the first step, consider Fig. 1a, in which the essential parameters are introduced. Using Newton's Second Law for motion along the lateral axis, one can obtain

$$m a_y(t) = F_f(t) + F_r(t) \tag{1}$$

in which

$$\begin{aligned} a_y(t) &= \dot{v}_y(t) + v_x\dot{\psi}(t) \\ F_f(t) &= f_{y_1}(t) = f_{y_2}(t) \\ F_r(t) &= f_{y_3}(t) = f_{y_4}(t) \end{aligned}$$

and a_y, v_y, v_x, m, $\dot{\psi}$, F_f and F_r are the lateral acceleration and velocity, longitudinal velocity, vehicle mass, yaw rate, the lateral tire forces of front and rear wheels, respectively. It is assumed that the longitudinal velocity is constant. In addition

$$I_z\ddot{\psi}(t) = l_f F_f(t) - l_r F_r(t) \tag{2}$$

where I_z, l_f and l_r are the yaw moment of inertia, and distance from the front and rear axle to the center of gravity as depicted in Fig. 1a.

Among different existing tire models (see for instance [32], [33] the model presented in [33], i. e. the Pacejka model, is chosen because it is more fitted with experimental data. According to Fig. 1b, the lateral tire forces can be written as (3) and (4), as shown at the bottom of the next page, and the side-slip angles are defined as:

$$\begin{aligned} &\alpha_i(t) \\ &= -\tan^{-1}\left(\frac{v_y(t)-(n_t\cos\delta(t))\dot{\delta}(t)-(n_t\cos\delta(t)-l_f)\dot{\psi}(t)}{v_x-(n_t\sin\delta(t))\dot{\delta}(t)-(n_t\sin\delta(t)+(-1)^i\frac{s_b}{2})\dot{\psi}(t)}\right) \\ &\quad +\delta(t) \end{aligned} \tag{5}$$

for $i = 1, 2$, and

$$\alpha_i(t) = -\tan^{-1}\left(\frac{v_y(t) - l_r\dot{\psi}(t)}{v_x + (-1)^i(\frac{s_b}{2})\dot{\psi}(t)}\right) \tag{6}$$

for $i = 3, 4$. In (5)-(6), n_t and s_b are tire-road length contact and tire-base, respectively, and b_i, c_i, d_i, and e_i are constants related to the tire characteristics, road, and vehicle operational condition. Moreover, it should be mentioned that the only control input in this problem is $\delta(t)$ which is the steering angle.

Since the derived model is so complex that its handling is intricate, some simplifications are introduced and thus, the following results can be obtained [34]:

$$F_f(t) = 2C_f(\delta(t) - \theta_f(t)) \tag{7}$$
$$F_r(t) = -2C_r\theta_r(t) \tag{8}$$
$$\theta_f(t) = \tan^{-1}\left(\frac{v_y(t) + l_f\dot{\psi}(t)}{v_x}\right) \tag{9}$$
$$\theta_r(t) = \tan^{-1}\left(\frac{v_y(t) - l_r\dot{\psi}(t)}{v_x}\right) \tag{10}$$

where θ_f, θ_r, C_f and C_r are the angles between the velocity vector and the longitudinal speed direction of front and rear tire, and the front and rear tire cornering stiffness, respectively. Using the obtained simplified formulas (7)-(10), vehicle lateral dynamics is reduced to

$$\begin{aligned}\dot{v}_y(t) &= -v_x\dot{\psi}(t) - \frac{2C_f}{m}\tan^{-1}\left(\frac{v_y(t) + l_f\dot{\psi}(t)}{v_x}\right) \\ &\quad - \frac{2C_r}{m}\tan^{-1}\left(\frac{v_y(t) - l_r\dot{\psi}(t)}{v_x}\right) + \frac{2C_f}{m}\delta(t) \\ \ddot{\psi}(t) &= -\frac{2C_f l_f}{I_z}\tan^{-1}\left(\frac{v_y(t) + l_f\dot{\psi}(t)}{v_x}\right) + \frac{2C_f l_f}{I_z}\delta(t) \\ &\quad + \frac{2C_r l_r}{I_z}\tan^{-1}\left(\frac{v_y(t) - l_r\dot{\psi}(t)}{v_x}\right)\end{aligned}$$

For the lane keeping purpose, two additional differential equations describing lateral deviation, y_L and tangent angle (heading error), ϵ_L are needed, which can be represented by [35]

$$\dot{y}_L(t) = v_y(t) + T_p v_x\dot{\psi}(t) + v_x\epsilon_L(t) \tag{11}$$
$$\dot{\epsilon}_L(t) = \dot{\psi}(t) - v_x\rho(t) \tag{12}$$

in which, ρ is the road curvature.

A. FORMAL STATEMENT OF PROBLEM

By defining $\mathbf{x} = [x_1(t) \;\; x_2(t) \;\; x_3(t) \;\; x_4(t)]^T = [v_y(t) \;\; \dot{\psi}(t) \;\; \epsilon_L(t) \;\; y_L(t)]^T$, consider the following dynamics of the vehicle

$$\begin{aligned}\dot{x}_1(t) &= -v_x x_2(t) - \frac{2C_f}{m}\tan^{-1}\left(\frac{x_1(t) + l_f x_2(t)}{v_x}\right) \\ &\quad - \frac{2C_r}{m}\tan^{-1}\left(\frac{x_1(t) - l_r x_2(t)}{v_x}\right) + \frac{2C_f}{m}u(t) \\ &\quad + \sum_{i=1}^{k} p_{i_1}(\mathbf{x})\omega_i(t) \end{aligned}\tag{13}$$

$$\begin{aligned}\dot{x}_2(t) &= -\frac{2C_f l_f}{I_z}\tan^{-1}\left(\frac{x_1(t) + l_f x_2(t)}{v_x}\right) \\ &\quad + \frac{2C_r l_r}{I_z}\tan^{-1}\left(\frac{x_1(t) - l_f x_2(t)}{v_x}\right) \\ &\quad + \frac{2C_f l_f}{I_z}u(t) + \sum_{i=1}^{k} p_{i_2}(\mathbf{x})\omega_i(t)\end{aligned}\tag{14}$$

$$\dot{x}_3(t) = x_1(t) + T_p v_x x_2(t) + v_x x_4(t) \tag{15}$$
$$\dot{x}_4(t) = x_2(t) - v_x\rho(t) + \sum_{i=1}^{k} p_{i_4}(\mathbf{x})\omega_i(t) \tag{16}$$
$$y(t) = h_x(\mathbf{x}(t)) = x_3(t) \tag{17}$$

in which $u(t) = \delta(t)$ and ω_i's are disturbances that originate from different sources, like uncertainty and variations in vehicle parameters, simplifications, and external disturbances like road bank angle and crosswinds. In the presence of these disturbances, ω_i's, the goal is to

1) Specify the maximum number of different classes of disturbances that can be decoupled from the lateral deviation as the output.
2) Design a disturbance decoupler to dissociate these disturbances from the output.
3) Design a tracking control law to track a reference path.

III. CONTROL DESIGN

In solving the aforementioned problem, we take two successive stages. The first step is designing a disturbance decoupler and after capturing this goal, we move to design the tracking mechanism. Prior to these two steps, the reference dynamics should be specified, so the following definition is presented.

Definition 1: The reference road curvature $\rho(t)$ is accessible if and only if there exists functions $x_{1_r}(t)$, $x_{2_r}(t)$, $x_{3_r}(t)$, $x_{4_r}(t)$ and $\delta_r(t)$ such that

$$\begin{aligned}\dot{x}_{1_r}(t) &= -v_x x_{2_r}(t) - \frac{2C_f}{m}\tan^{-1}\left(\frac{x_{1_r}(t) + l_f x_{2_r}(t)}{v_x}\right) \\ &\quad - \frac{2C_r}{m}\tan^{-1}\left(\frac{x_{1_r}(t) - l_r x_{2_r}(t)}{v_x}\right) + \frac{2C_f}{m}\delta_r(t) \\ \dot{x}_{2_r}(t) &= -\frac{2C_f l_f}{I_z}\tan^{-1}\left(\frac{x_{1_r}(t) + l_f x_{2_r}(t)}{v_x}\right) \\ &\quad + \frac{2C_r l_r}{I_z}\tan^{-1}\left(\frac{x_{1_r}(t) - l_r x_{2_r}(t)}{v_x}\right) + \frac{2C_f l_f}{I_z}\delta_r(t) \\ \dot{x}_{3_r}(t) &= x_{1_r}(t) + L x_{2_r}(t) + v_x x_{4_r}(t) \\ \dot{x}_{4_r}(t) &= x_{2_r}(t) - v_x\rho(t) \\ y_r(t) &= x_{3_r}(t)\end{aligned}\tag{18}$$

$$F_f(t) = \sum_{i=1}^{2} d_i \sin\left(c_i \tan^{-1}\left(b_i(1 - e_i)\alpha_i(t) + e_i \tan^{-1}(b_i\alpha_i(t))\right)\right) \tag{3}$$
$$F_r(t) = \sum_{i=3}^{4} d_i \sin\left(c_i \tan^{-1}\left(b_i(1 - e_i)\alpha_i(t) + e_i \tan^{-1}(b_i\alpha_i(t))\right)\right) \tag{4}$$

Introducing new functions

$$\Psi_-(z_1,w_1,z_2,w_2) = 1 + (\frac{z_1 - l_r w_1}{v_x})(\frac{z_2 - l_r w_2}{v_x}) + (\frac{z_2 - l_r w_2}{v_x})^2$$
$$\Psi_+(z_1,w_1,z_2,w_2) = 1 + (\frac{z_1 + l_f w_1}{v_x})(\frac{z_2 + l_f w_2}{v_x}) + (\frac{z_2 + l_f w_2}{v_x})^2$$

and utilizing the overall and reference dynamics (13)-(16) and (18), the error dynamics becomes

$$\begin{aligned}
\dot{x}_{1_e}(t) &= -\frac{2C_f}{m}\tan^{-1}\left(\frac{\frac{x_{1_e}(t)+l_f x_{2_e}(t)}{v_x}}{\Psi_+(x_{1_e},x_{2_e},x_{1_r},x_{2_r})}\right) - \frac{2C_r}{m}\tan^{-1}\left(\frac{\frac{x_{1_e}(t)-l_r x_{2_e}(t)}{v_x}}{\Psi_-(x_{1_e},x_{2_e},x_{1_r},x_{2_r})}\right) \\
&\quad - v_x x_{2_e}(t) + \frac{2C_f}{m}\delta_e(t) + \sum_{i=1}^{k} p_{i_1}(\mathbf{x})\omega_i(t) \\
\dot{x}_{2_e}(t) &= -\frac{2C_f l_f}{I_z}\tan^{-1}\left(\frac{\frac{x_{1_e}(t)+l_f x_{2_e}(t)}{v_x}}{\Psi_+(x_{1_e},x_{2_e},x_{1_r},x_{2_r})}\right) + \frac{2C_r l_r}{I_z}\tan^{-1}\left(\frac{\frac{x_{1_e}(t)-l_r x_{2_e}(t)}{v_x}}{\Psi_-(x_{1_e},x_{2_e},x_{1_r},x_{2_r})}\right) \\
&\quad + \frac{2C_f l_f}{I_z}\delta_e(t) + \sum_{i=1}^{k} p_{i_2}(\mathbf{x})\omega_i(t) \\
\dot{x}_{3_e}(t) &= x_{1_e}(t) + L x_{2_e}(t) + v_x x_{4_e}(t) \\
\dot{x}_{4_e}(t) &= x_{2_e}(t) + \sum_{i=1}^{k} p_{i_4}(\mathbf{x})\omega_i(t)
\end{aligned} \tag{19}$$

Introducing new variables $[\eta_1(t),\ \eta_2(t),\ \eta_3(t),\ \eta_4(t)] = [\frac{x_1(t)+l_f x_2(t)}{v_x},\ \frac{x_1(t)-l_r x_2(t)}{v_x},\ x_3(t),\ x_4(t)]$, corresponding reference and error variables

$$\eta_{1_r}(t) = \frac{x_{1_r}(t) + l_f x_{2_r}(t)}{v_x}, \quad \eta_{3_r}(t) = x_{3_r}(t) \tag{20a}$$
$$\eta_{2_r}(t) = \frac{x_{1_r}(t) - l_r x_{2_r}(t)}{v_x}, \quad \eta_{4_r}(t) = x_{4_r}(t) \tag{20b}$$

and

$$\eta_{1_e}(t) = \frac{x_{1_e}(t) + l_f x_{2_e}(t)}{v_x}, \quad \eta_{3_e}(t) = x_{3_e}(t) \tag{21a}$$
$$\eta_{2_e}(t) = \frac{x_{1_e}(t) - l_r x_{2_e}(t)}{v_x}, \quad \eta_{4_e}(t) = x_{4_e}(t) \tag{21b}$$

the error dynamics (19) reduces to

$$\begin{aligned}
\dot{\eta}_{1_e}(t) &= k(\eta_1(t) - \eta_2(t)) + \gamma_1 \tan^{-1}\left(\frac{\eta_{2_e}(t)}{1+\eta_2(t)\eta_{2_r}(t)}\right) - \beta_1 \tan^{-1}\left(\frac{\eta_{1_e}(t)}{1+\eta_1(t)\eta_{1_r}(t)}\right) + \beta_1 u_e(t) + \sum_{i=1}^{k} q_{i_1}(\eta)\omega_i(t) \\
\dot{\eta}_{2_e}(t) &= k(\eta_1(t) - \eta_2(t)) + \gamma_2 \tan^{-1}\left(\frac{\eta_{2_e}(t)}{1+\eta_2(t)\eta_{2_r}(t)}\right) - \beta_2 \tan^{-1}\left(\frac{\eta_{1_e}(t)}{1+\eta_1(t)\eta_{1_r}(t)}\right) + \beta_2 u_e(t) + \sum_{i=1}^{k} q_{i_2}(\eta)\omega_i(t) \\
\dot{\eta}_{3_e}(t) &= -k(L+l_r)\eta_{1_e}(t) + k(L-l_f)\eta_{2_e}(t) + v_x\eta_{4_e}(t) \\
\dot{\eta}_{4_e}(t) &= -k\eta_{1_e}(t) + k\eta_{2_e}(t) + \sum_{i=1}^{k} q_{i_4}(\eta)\omega_i(t) \\
y_e(t) &= h_\eta(t) = \eta_{3_e}(t)
\end{aligned} \tag{22}$$

where

$$k = \frac{-v_x}{l_f + l_r}, \quad \gamma_1 = \frac{2C_r l_f l_r}{I_z v_x} - \frac{2C_r}{m v_x}, \quad \beta_1 = \frac{2C_f l_f^2}{I_z v_x} + \frac{2C_f}{m v_x}, \quad \gamma_2 = \frac{-2C_r l_r^2}{I_z v_x} - \frac{2C_r}{m v_x}, \quad \beta_2 = \frac{2C_f}{m v_x} - \frac{2C_f l_f l_r}{I_z v_x}$$

Moreover, this dynamics can be compactly rewritten as

$$\dot{\boldsymbol{\eta}}_e = \mathbf{f}(\boldsymbol{\eta}_e, \boldsymbol{\eta}_r) + \mathbf{g}(\boldsymbol{\eta}_e)u_e + \mathbf{p}(\boldsymbol{\eta}_e)\boldsymbol{\omega} \tag{23}$$

In the proceeding, the mentioned two successive steps are applied to the error dynamics (22). In addition, time dependence is dropped for simplicity.

A. DISTURBANCE DECOUPLING

Considering the error dynamics (22), a steering control law of the following form is sought

$$u_e(\boldsymbol{\eta}_e, \boldsymbol{\eta}_r) = \lambda(\boldsymbol{\eta}_e, \boldsymbol{\eta}_r) + \mu(\boldsymbol{\eta}_e).\nu(\boldsymbol{\eta}_e) \tag{24}$$

in which $\lambda(\boldsymbol{\eta}_e, \boldsymbol{\eta}_r)$ and $\mu(\boldsymbol{\eta})$ are unknown and have to be computed. In addition, the auxiliary control $\nu(\boldsymbol{\eta}_e)$ is used for other purposes like stabilizing. Utilizing (24), the closed-loop control system (23) can be decomposed to two subsystems as follows

$$\begin{aligned}
\dot{\boldsymbol{\zeta}}_1 &= \mathbf{f}_{d_1}(\boldsymbol{\zeta}_1, \boldsymbol{\zeta}_2) + \mathbf{g}_{d_1}(\boldsymbol{\zeta}_1, \boldsymbol{\zeta}_2)\nu + \mathbf{q}_{d_1}(\boldsymbol{\zeta}_1, \boldsymbol{\zeta}_2)\boldsymbol{\omega} \\
\dot{\boldsymbol{\zeta}}_2 &= \mathbf{f}_{d_2}(\boldsymbol{\zeta}_2) + \mathbf{g}_{d_2}(\boldsymbol{\zeta}_2)\nu \\
y &= h_\zeta(\zeta_2)
\end{aligned}$$

where $\boldsymbol{\zeta}_1 \in \mathcal{X}_{\zeta_1} \subset \mathbb{R}^{n_1}$, $\boldsymbol{\zeta}_2 \in \mathcal{X}_{\zeta_2} \subset \mathbb{R}^{n_2}$ in which $n_2 \geq 1$, $\mathbf{f}_{d_1} \in \mathcal{X}_{f_{d_1}} \subset \mathbb{R}^{n_1}$, $\mathbf{g}_{d_1} \in \mathcal{X}_{g_{d_1}} \subset \mathbb{R}^{n_1}$, $\mathbf{q}_{d_1} \in \mathcal{X}_{p_{d_1}} \subset \mathbb{R}^{n_1\times\kappa}$, $\boldsymbol{\omega} \in \mathbb{R}^{\kappa}$, $\mathbf{f}_{d_2} \in \mathcal{X}_{f_{d_2}} \subset \mathbb{R}^{n_2}$, $\mathbf{g}_{d_2} \in \mathcal{X}_{g_{d_2}} \subset \mathbb{R}^{n_2}$ and $n_1 + n_2 = 4$. From geometrical point of view, it can be interpreted that if two initial points $\mathbf{x}_1(t_0)$ and $\mathbf{x}_2(t_0)$ are chosen on the manifold $\boldsymbol{\zeta}_2(t_0) = C_1$, after $T - t_0$ seconds with same control input $u(t)$, the two outputs, $h_1(\boldsymbol{\zeta}_2)$ and $h_2(\boldsymbol{\zeta}_2)$, will be the same because $\mathbf{x}_{4,1}(T)$ and $\mathbf{x}_{4,2}(T)$ both lie on the manifold $\zeta_2(T) = C_2$ whereas their corresponding trajectories are not necessarily the same, as demonstrated in Fig. 2. Consequently, manifold $\mathcal{M}_i$, for $i \in \mathbb{N}$, is an unobservable space of the system with respect to disturbance input and is defined as

$$\mathcal{M}_i(t^*) := \{\mathbf{x}(t^*) \in \mathbb{R}^n | \zeta_2(t^*) = C_i = \text{constant}\} \tag{25}$$

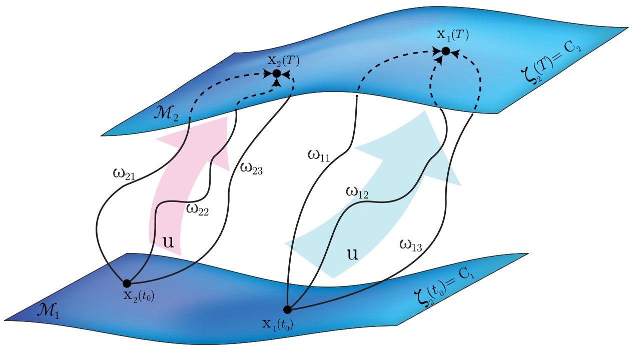

FIGURE 2. Unobservable space with respect to disturbance input.

Since the subsystem $\boldsymbol{\zeta}_2$ is not affected by the disturbance $\boldsymbol{\omega}$, it should be in a space that is perpendicular to space spanned by vectors $\mathbf{q}(\boldsymbol{\eta})$. Because it is desired to decouple the disturbance with maximum components from the output, the dimension of the unobservable space of system (23) should be minimized. A space spanned by the vectors $\mathbf{q}(\boldsymbol{\eta})$ with maximum dimension should be sought. It is clear that the mentioned spanned set is uniquely characterized by its orthogonal complement. For this purpose, an algorithm has been introduced [36], [37]:

$$\begin{aligned} \Omega_0 &= \mathrm{d}h_{\eta_e} \\ \Omega_k &= \Omega_{k-1} + L_f\Big(\Omega_{k-1} \cap G^{\perp}\Big) + L_g\Big(\Omega_{k-1} \cap G^{\perp}\Big) \end{aligned} \tag{26}$$

where $G = \text{span}(g)$. It has been shown that there exists σ^*, for $\sigma > \sigma^*$ we have $\Omega_\sigma = \Omega_{\sigma-1}$ and we take $\Omega^* = \Omega_{\sigma^*}$. In addition, for every $\boldsymbol{\psi}_i \in \Omega^*$ we have

$$\prec \boldsymbol{\psi}_i^T, \mathbf{f}(\boldsymbol{\eta}_e, \boldsymbol{\eta}_r) + \mathbf{g}(\boldsymbol{\eta}_e)\lambda(\boldsymbol{\eta}_e, \boldsymbol{\eta}_r) \succ = 0 \tag{27}$$

$$\prec \boldsymbol{\psi}_i^T, \mathbf{g}(\boldsymbol{\eta}_e)\mu(\boldsymbol{\eta}_e) \succ = \delta_{i1} \tag{28}$$

in which

$$\delta_{ij} = \begin{cases} 1 & \text{if } i = j \\ 0 & \text{if } i \neq j \end{cases}$$

Recalling dynamics (22) and using algorithm (26), one can obtain:

$$\begin{aligned} \Omega_0 &= \text{span}\Big\{[0\ 0\ 1\ 0]\Big\} \\ G &= \text{span}\Big\{[\beta_1\ \beta_2\ 0\ 0]\Big\} \end{aligned}$$

As a result

$$\begin{aligned} G^{\perp} &= \text{span}\Big\{[0\ 0\ 1\ 0], [0\ 0\ 0\ 1], [-\beta_2\ \beta_1\ 0\ 0]\Big\} \\ \Omega_0 \cap G^{\perp} &= \Omega_0 \end{aligned} \tag{29}$$

Moreover

$$\begin{aligned} L_f\Big(\Omega_0 \cap G^{\perp}\Big) &= \text{span}\Big\{[0\ 0\ 1\ 1]\frac{\partial}{\partial \boldsymbol{\eta}_e}\Upsilon(\boldsymbol{\eta})\Big\} \\ &= \text{span}\Big\{\boldsymbol{v}_p\Big\} \end{aligned}$$

in which

$$\Upsilon(\boldsymbol{\eta}) = \begin{bmatrix} k(\eta_1 - \eta_2) + \gamma_1 \tan^{-1}\Big(\dfrac{\eta_{2_e}}{1 + \eta_2\eta_{2_r}}\Big) \\ -\beta_1 \tan^{-1}\Big(\dfrac{\eta_{1_e}}{1 + \eta_1\eta_{1_r}}\Big) \\ k(\eta_1 - \eta_2) + \gamma_2 \tan^{-1}\Big(\dfrac{\eta_{2_e}}{1 + \eta_2\eta_{2_r}}\Big) \\ -\beta_2 \tan^{-1}\Big(\dfrac{\eta_{1_e}}{1 + \eta_1\eta_{1_r}}\Big) \\ -k(L + l_r)\eta_{1_e} + k(L - l_f)\eta_{2_e} + v_x\eta_{4_e} \\ -k\eta_{1_e} + k\eta_{2_e} \end{bmatrix}$$

and

$$\boldsymbol{v}_p = [-k(L + l_r)\ \ k(L - l_f)\ \ 0\ v_x] \tag{30}$$

In a similar manner

$$L_g\Big(\Omega_0 \cap G^{\perp}\Big) = \emptyset \tag{31}$$

thus

$$\begin{aligned} \Omega_1 &= \Omega_0 + L_f\Big(\Omega_0 \cap G^{\perp}\Big) + L_g\Big(\Omega_0 \cap G^{\perp}\Big) \\ &= \text{span}\Big\{[0\ 0\ 1\ 0], \boldsymbol{v}_p\Big\} \end{aligned} \tag{32}$$

According to (29) and (32), if condition

$$\frac{\beta_2}{k(L + l_r)} \neq \frac{\beta_1}{k(L - l_f)} \tag{33}$$

satisfies, then $\Omega_0 = \Omega_1 \cap G^{\perp}$ and the following results hold

$$\begin{aligned} \Omega_2 &= \Omega_1 + L_f\Big(\Omega_1 \cap G^{\perp}\Big) + L_g\Big(\Omega_1 \cap G^{\perp}\Big) \\ &= \Omega_1 + L_f\Big(\Omega_0\Big) + L_g\Big(\Omega_0\Big) \\ &= \Omega_1 \end{aligned}$$

Consequently $\Omega_1 = \Omega^*$, and

$$\begin{aligned} &\Omega^{*^{\perp}} \\ &= \text{span}\Big\{[L - l_f\ \ L + l_r\ \ 0\ \ 0]^T, [0\ \ -v_x\ \ 0\ \ k(L - l_f)]^T\Big\} \end{aligned} \tag{34}$$

Finally, all classes of decouplable disturbances from the desired output can be demonstrated as follows

$$\begin{aligned} \dot{\eta}_{1_e} &= f_1(\boldsymbol{\eta}_e, \boldsymbol{\eta}_r) + g_1(\boldsymbol{\eta}_e)u_e + (L - l_f)\omega_1 \\ \dot{\eta}_{2_e} &= f_2(\boldsymbol{\eta}_e, \boldsymbol{\eta}_r) + g_2(\boldsymbol{\eta}_e)u_e + (L + l_r)\omega_1 - v_x\omega_2 \\ \dot{\eta}_{3_e} &= f_3(\boldsymbol{\eta}_e) + g_3(\boldsymbol{\eta}_e)u_e \\ \dot{\eta}_{4_e} &= f_4(\boldsymbol{\eta}_e) + g_4(\boldsymbol{\eta}_e)u_e + k(L - l_f)\omega_2 \\ y_e &= \eta_{3_e} \end{aligned}$$

To find a decoupling controller, it is assumed that $\mathbf{f}(\boldsymbol{\eta}_e, \boldsymbol{\eta}_r) + \mathbf{g}(\boldsymbol{\eta}_e)\lambda(\boldsymbol{\eta}_e, \boldsymbol{\eta}_r)$ and $\mathbf{g}(\boldsymbol{\eta}_e)\mu(\boldsymbol{\eta}_e)$ are in a proper Hilbert space $\mathcal{H}_1 \subset \mathbb{R}^4$. Moreover, $\lambda(\boldsymbol{\eta}_e, \boldsymbol{\eta}_r)$ and $\mu(\boldsymbol{\eta}_e)$ are in another proper Hilbert space $\mathcal{H}_2 \subset \mathbb{R}$. If $\psi \in \Omega^*$, using control invariant property of $\Omega^{*^\perp}$, one can obtain

$$\prec \psi^T, \mathbf{f}(\boldsymbol{\eta}_e, \boldsymbol{\eta}_r) + \mathbf{g}(\boldsymbol{\eta}_e)\lambda(\boldsymbol{\eta}_e, \boldsymbol{\eta}_r) \succ = 0$$

which directly results in

$$\mathrm{Conj}(\lambda(\boldsymbol{\eta}_e, \boldsymbol{\eta}_r)) = -\frac{\prec \psi^T, \mathbf{f}(\boldsymbol{\eta}_e, \boldsymbol{\eta}_r) \succ}{\prec \psi^T, \mathbf{g}(\boldsymbol{\eta}_e) \succ} \tag{35}$$

in which $\mathrm{Conj}(\lambda(\boldsymbol{\eta}_e, \boldsymbol{\eta}_r))$ is the complex conjugate of $\lambda(\boldsymbol{\eta}_e, \boldsymbol{\eta}_r)$.

Remark 2: $\lambda(\boldsymbol{\eta}_e, \boldsymbol{\eta}_r)$ is well-defined and as a result, the denominator cannot be zero

Now, according to (27) and (28), we approach to compute unknown coefficients, $\lambda(\boldsymbol{\eta}_e, \boldsymbol{\eta}_r)$ and $\mu(\boldsymbol{\eta}_e)$:

$$\prec \mathbf{v}_p\ ,\ \mathbf{f}(\boldsymbol{\eta}_e, \boldsymbol{\eta}_r) + \mathbf{g}(\boldsymbol{\eta}_e)\lambda(\boldsymbol{\eta}_e, \boldsymbol{\eta}_r) \succ\ = 0 \tag{36a}$$

$$\prec \mathbf{v}_p\ ,\ \mathbf{g}(\boldsymbol{\eta}_e)\mu(\boldsymbol{\eta}_e) \succ\ = 1 \tag{36b}$$

Remark 3: If the inner product in (35) and (36) on the Hilbert space $\mathcal{H}_1$ be the Euclidean product, one can conclude

$$\lambda(\boldsymbol{\eta}_e, \boldsymbol{\eta}_r) = \frac{k(L+l_r)f_1(\boldsymbol{\eta}_e, \boldsymbol{\eta}_r) - k(L-l_f)f_2(\boldsymbol{\eta}_e, \boldsymbol{\eta}_r) - v_x f_4(\boldsymbol{\eta}_e)}{-k\beta_1(L+l_r) + k\beta_2(L-l_f)} \tag{37}$$

and

$$\mu(\boldsymbol{\eta}_e) = \frac{1}{-k\beta_1(L+l_r) + k\beta_2(L-l_f)} = \frac{1}{d} \tag{38}$$

Therefore, the control law becomes $u_e(\boldsymbol{\eta}_e, \boldsymbol{\eta}_r) = \lambda(\boldsymbol{\eta}_e, \boldsymbol{\eta}_r) + \mu(\boldsymbol{\eta}_e).\nu(\boldsymbol{\eta}_e)$.

Remark 4: According to condition (33), the denominators of $\lambda(\boldsymbol{\eta}_e, \boldsymbol{\eta}_r)$ and $\mu(\boldsymbol{\eta}_e)$ are nonzero.

Using (20) and (21), the control input (24) can be obtained in terms of $\mathbf{x}_e$:

$$\lambda(\mathbf{x}_e, \mathbf{x}_r) = \frac{k(L+l_r)\acute{f}_1(\mathbf{x}_e, \mathbf{x}_r) - k(L-l_f)\acute{f}_2(\mathbf{x}_e, \mathbf{x}_r) - v_x \acute{f}_4(\mathbf{x}_e)}{-k\beta_1(L+l_r) + k\beta_2(L-l_f)} \tag{39}$$

and

$$\mu(\mathbf{x}_e) = \frac{1}{-k\beta_1(L+l_r) + k\beta_2(L-l_f)} = \frac{1}{d} \tag{40}$$

in which

$$\begin{aligned}
\acute{f}_1(\mathbf{x}_e, \mathbf{x}_r) &= -x_{2_e} - \beta_1 \tan^{-1}\left(\frac{\frac{x_{1_e} + l_f x_{2_e}}{v_x}}{\Psi_+(x_{1_e}, x_{2_e}, x_{1_r}, x_{2_r})}\right) \\
&\quad + \gamma_1 \tan^{-1}\left(\frac{\frac{x_{1_e} - l_r x_{2_e}}{v_x}}{\Psi_-(x_{1_e}, x_{2_e}, x_{1_r}, x_{2_r})}\right) \\
\acute{f}_2(\mathbf{x}_e, \mathbf{x}_r) &= -x_{2_e} - \beta_2 \tan^{-1}\left(\frac{\frac{x_{1_e} + l_f x_{2_e}}{v_x}}{\Psi_+(x_{1_e}, x_{2_e}, x_{1_r}, x_{2_r})}\right) \\
&\quad + \gamma_2 \tan^{-1}\left(\frac{\frac{x_{1_e} - l_r x_{2_e}}{v_x}}{\Psi_-(x_{1_e}, x_{2_e}, x_{1_r}, x_{2_r})}\right)
\end{aligned}$$

$$\acute{f}_4(\mathbf{x}_e) = -x_{2_e}.$$

B. DESIGNING A STABILIZER

From now on, we take the second step, namely designing the stabilizing mechanism for the error dynamics by assuming that the disturbances have been decoupled from the output. The stabilizing control law, $\nu(\boldsymbol{\eta}_e)$, should contain disturbance-free terms to retain the output decoupled from the disturbances. For this purpose, it is assumed that $\nu(\boldsymbol{\eta}_e)$ has the following form

$$\begin{aligned}
\nu(\boldsymbol{\eta}_e) &= c_1\eta_{3_e} + c_2 f_3(\boldsymbol{\eta}_e) \\
&= c_1\eta_{3_e} + c_2\Big(-k(L+l_r)\eta_{1_e} \\
&\qquad + k(L-l_f)\eta_{2_e} + v_x\eta_{4_e}\Big)
\end{aligned} \tag{41}$$

and in terms of $\boldsymbol{x}_e$

$$\nu(\mathbf{x}_e) = c_1 x_{3_e} + c_2\Big(x_{1_e} + T_p v_x x_{2_e} + v_x x_{4_e}\Big) \tag{42}$$

The coefficients c_1 and c_2 should be determined in such a way to stabilize the error dynamics (22). Substituting $\lambda(\boldsymbol{\eta}_e)$ (37), $\mu(\boldsymbol{\eta}_e)$ (38) and $\nu(\boldsymbol{\eta}_e)$ (41) in error dynamics (22), it can be shown that $\mathbf{f}(\boldsymbol{\eta}_e, \boldsymbol{\eta}_r)$ in (23) can be written as

$$\dot{\boldsymbol{\eta}}_e = \mathbf{f}_{cl}(\boldsymbol{\eta}_e, \boldsymbol{\eta}_r) + \mathbf{p}(\boldsymbol{\eta}_e)\boldsymbol{\omega} \tag{43}$$

in which

$$\mathbf{f}_{cl}(\boldsymbol{\eta}_e, \boldsymbol{\eta}_r) = \Big(A + \boldsymbol{\phi}_1(\boldsymbol{\eta}_e, \boldsymbol{\eta}_r) + \boldsymbol{\phi}_2(\boldsymbol{\eta}_r)\Big)\boldsymbol{\eta}_e \tag{44}$$

where A, (45), is introduced at the shown at the bottom of the next page, and

$$\boldsymbol{\phi}_1(\boldsymbol{\eta}_e, \boldsymbol{\eta}_r) = \begin{bmatrix} \acute{\beta}_1\Lambda(\eta_{1_e}, \eta_{1_r}) & -\acute{\gamma}_1\Lambda(\eta_{2_e}, \eta_{2_r}) & \mathbf{0}_{1\times2} \\ \acute{\beta}_2\Lambda(\eta_{1_e}, \eta_{1_r}) & -\acute{\gamma}_2\Lambda(\eta_{2_e}, \eta_{2_r}) & \mathbf{0}_{1\times2} \\ \mathbf{0}_{2\times1} & \mathbf{0}_{2\times1} & \mathbf{0}_{2\times2} \end{bmatrix}$$

$$\boldsymbol{\phi}_2(\boldsymbol{\eta}_r) = \begin{bmatrix} \acute{\beta}_1\dfrac{\eta_{1_r}^2}{1+\eta_{1_r}^2} & -\acute{\gamma}_1\dfrac{\eta_{2_r}^2}{1+\eta_{2_r}^2} & \mathbf{0}_{1\times2} \\ \acute{\beta}_2\dfrac{\eta_{1_r}^2}{1+\eta_{1_r}^2} & -\acute{\gamma}_2\dfrac{\eta_{2_r}^2}{1+\eta_{2_r}^2} & \mathbf{0}_{1\times2} \\ \mathbf{0}_{2\times1} & \mathbf{0}_{2\times1} & \mathbf{0}_{2\times2} \end{bmatrix} \tag{46}$$

such that

$$\begin{aligned}
\Lambda(z, w) &= \frac{1}{1+w^2} - \frac{\tan^{-1}(\frac{z}{1+(z+w)w})}{z} \\
\acute{k}_1 &= k + \beta_1 k^2\frac{L+l_r}{d} - \beta_1 k^2\frac{L-l_f}{d} + k\beta_1\frac{v_x}{d} \\
\acute{\beta}_1 &= \beta_1 + k\beta_1^2\frac{L+l_r}{d} - k\beta_1\beta_2\frac{L-l_f}{d} \\
\acute{\gamma}_1 &= \gamma_1 + k\gamma_1\beta_1\frac{L+l_r}{d} - k\beta_1\gamma_2\frac{L-l_f}{d} \\
\acute{k}_2 &= k + \beta_2 k^2\frac{L+l_r}{d} - \beta_2 k^2\frac{L-l_f}{d} + k\beta_2\frac{v_x}{d} \\
\acute{\beta}_2 &= \beta_2 + k\beta_1\beta_2\frac{L+l_r}{d} - k\beta_2^2\frac{L-l_f}{d} \\
\acute{\gamma}_2 &= \gamma_2 + k\gamma_1\beta_2\frac{L+l_r}{d} - k\beta_2\gamma_2\frac{L-l_f}{d}
\end{aligned}$$

Since

$$\lim_{\eta_{i_e}\to 0} \frac{\tan^{-1}(\frac{\eta_{i_e}}{1+\eta_i\eta_{i_r}})}{\eta_{i_e}} = \frac{1}{1+\eta_{i_r}^2}$$

it can be concluded that

$$\lim_{\boldsymbol{\eta}_e\to\mathbf{0}} \boldsymbol{\phi}_1(\boldsymbol{\eta}_e, \boldsymbol{\eta}_r) = \mathbf{0}$$

Remark 5: Since $\boldsymbol{\phi}_2(\boldsymbol{\eta}_r)$ is bounded and A is a constant matrix of coefficients c_1 and c_2, these parameters can be chosen such that $A+\boldsymbol{\phi}_2(\boldsymbol{\eta}_r)$ becomes Hurwitz for every $t \geq 0$. Because $\boldsymbol{\eta}_e = \mathbf{0}$ is an equilibrium point for the nonlinear system $\dot{\boldsymbol{\eta}}_e = \mathbf{f}_{cl}(\boldsymbol{\eta}_e, \boldsymbol{\eta}_r)$, and $\mathbf{f}_{cl}(\boldsymbol{\eta}_e, \boldsymbol{\eta}_r)$ is differentiable in a neighborhood of the origin, if c_1 and c_2 in (41) are chosen such that the matrix $A + \boldsymbol{\phi}_2(\boldsymbol{\eta}_r)$ becomes Hurwitz, then the origin becomes exponentially stable for the nonlinear system $\dot{\boldsymbol{\eta}}_e = \mathbf{f}_{cl}(\boldsymbol{\eta}_e, \boldsymbol{\eta}_r)$ [38]. Although in the presence of the disturbances, the exponential stability of the origin of the system (43) cannot be guaranteed, using robust methods, the stability of the origin can be investigated. The schematic of the controller is demonstrated in Fig. 3.

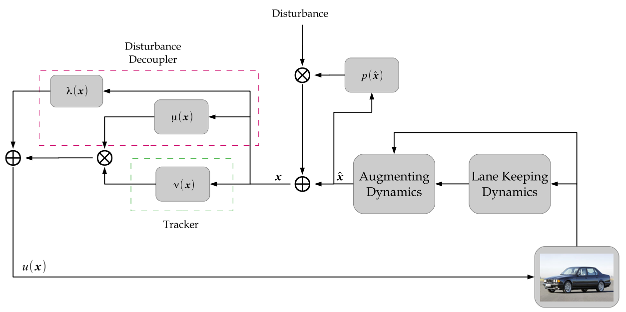

FIGURE 3. Schematic of the control design.

Finally, the obtained results are summarized in the following theorem:

Theorem 6: Consider the augmented lateral vehicle and lane keeping dynamics (13)-(16) with the lateral deviation (17) as an output. If the road curvature $\rho(t)$ is accessible, dynamics (13)-(16) could exponentially track their references in the absence of the disturbances with the control input

$$u(\mathbf{x}) = u_r(\mathbf{x}_r) + \lambda(\mathbf{x}_e) + \mu(\mathbf{x}_e).\nu(\mathbf{x}_e) \tag{47}$$

where $\lambda(\mathbf{x}_e)$, $\mu(\mathbf{x}_e)$, and $\nu(\mathbf{x}_e)$ are obtained in (39), (40) and (42), respectively. If disturbances of the form (34) are applied to the mentioned dynamics, control input (47) decouples the lateral deviation of the vehicle from the disturbances and ensures the stability of the error dynamics (22) by choosing proper c_1 and c_2 in (42) which make the matrix $A + \boldsymbol{\phi}_2(\boldsymbol{\eta}_r)$ Hurwitz.

IV. ILLUSTRATIVE EXAMPLES

In this section, the obtained tracking and disturbance decoupling controller is implemented on a typical vehicle introduced in [39] with parameters $m = 1421$ kg, $I_z = 2570$ kg.m^2, $l_f = 1.195$ m, $l_r = 1.513$ m, $C_f = 170550\ \frac{\text{N}}{\text{rad}}$ and $C_r = 137844\ \frac{\text{N}}{\text{rad}}$. Two cases with both uniformly distributed and exponentially attenuated disturbances are considered. Moreover, the effect of coefficients c_1 and c_2 in (41) on the behavior of states is investigated. In all cases, the reference path is considered to be a tortuous path with $\rho(t) = 0.05t$ and longitudinal velocity, v_x is assumed to be constant and equals to $10\frac{\text{m}}{\text{s}}$. Initial states are $[x_1,\ x_2,\ x_3,\ x_4] = [0.1,\ 0.2,\ 15,\ 0.4]$ and as can be seen, it is assumed that the vehicle is 15 meters apart from the reference path at the beginning.

A. UNIFORMLY DISTRIBUTED DISTURBANCES

In this case, ω_1 and ω_2 are uniformly distributed on the intervals [0, 0.5] and [0, 1], respectively and $c_1 = -5$ and $c_2 = -10$. As illustrated in Fig. 4, in the absence of the mentioned disturbances, the origin of the error dynamics is exponentially stable and the states track their references.

When the disturbances are applied, none of the states can track their references, except the third one, the lateral deviation, which is decoupled from the disturbances. As can be seen in Fig. 4c, y_L's in the presence and absence of the disturbances are the same.

The control input in two different situations, with and without disturbances, is shown in Fig. 5. In addition, the eigenvalues of the matrix $A + \boldsymbol{\phi}_2(\boldsymbol{\eta}_r)$ are depicted in Fig. 6, which demonstrates that the real parts of the eigenvalues remain negative in all the time.

B. EXPONENTIALLY ATTENUATED DISTURBANCES

In this case, $\omega_1 = \exp(-0.2t)\cos(400t)$, $\omega_2 = \exp(-0.4t)\sin(600t)$, $c_1 = -5$ and $c_2 = -10$. As demonstrated in Fig. 7, the error states exponentially converge to zero and when the disturbances diminish to zero, after about 16 seconds, all the states track their references. The disturbances have no effect on the third state, lateral deviation, as can be seen in Fig. 7c. In this figure, the left axes are corresponding to both the actual and reference states, while the

$$A = \begin{bmatrix} \acute{k}_1 - \acute{\beta}_1 - \frac{k\beta_1 c_2(L+l_r)}{d} & \acute{\gamma}_1 - \acute{k}_1 + \frac{k\beta_1 c_2(L-l_f)}{d} & \frac{\beta_1 c_1}{d} & \frac{\beta_1 c_1 v_x}{d} \\ \acute{k}_2 - \acute{\beta}_2 - \frac{k\beta_2 c_2(L+l_r)}{d} & \acute{\gamma}_2 - \acute{k}_2 + \frac{k\beta_2 c_2(L-l_f)}{d} & \frac{\beta_2 c_1}{d} & \frac{\beta_2 c_1 v_x}{d} \\ -k(L+l_r) & k(L-l_f) & 0 & v_x \\ -k & k & 0 & 0 \end{bmatrix} \tag{45}$$

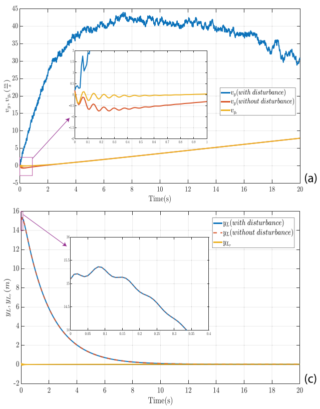

FIGURE 4. State variables in the presence and absence of the disturbances.

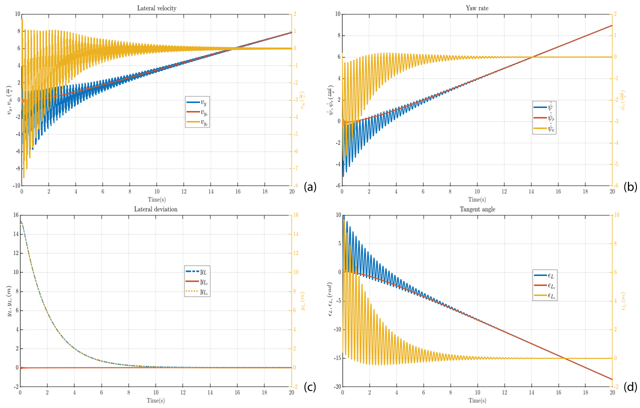

FIGURE 7. State variables in the presence and absence of the disturbances.

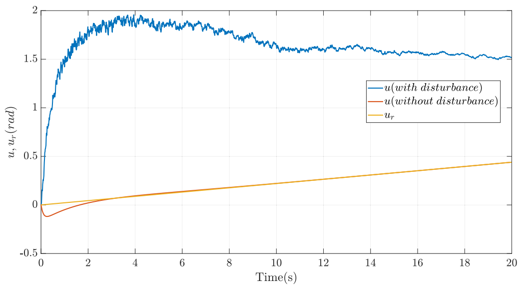

FIGURE 5. Control input in the presence and absence of the disturbances.

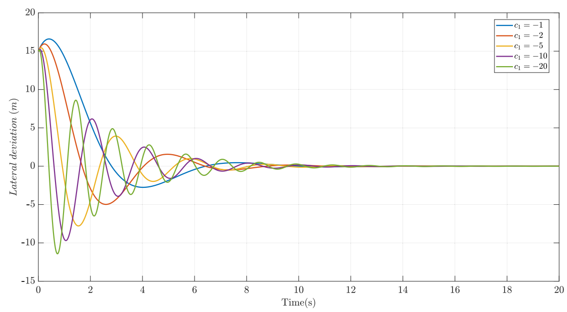

FIGURE 8. The effect of changing c_1 on the lateral deviation.

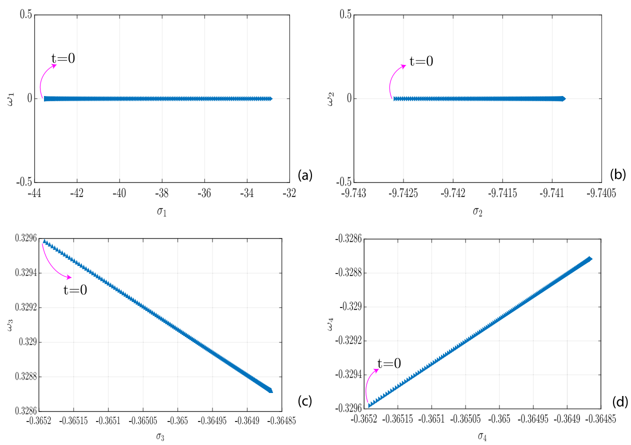

FIGURE 6. The eigenvalues of the matrix $A + \phi_2(\eta_r)$.

right axes are corresponding to the error states. In addition, since all the parameters in the previous and current subsection are the same and just their disturbances are different, the lateral deviation in Fig. 4c, and Fig. 7c, are identical.

C. THE EFFECT OF CHANGING COEFFICIENTS c_1 AND c_2

In this case, the effect of coefficients c_1 and c_2 on the lateral deviation is investigated. At first, it is assumed that $c_2 = -1$ and c_1 get different values. As can be seen in Fig. 8, decreasing c_1 from -1 to -20, increase the frequency of oscillation of the lateral deviation around its equilibrium point, but the settling time remains constant.

As shown in Fig. 9a, when $c_1 = -5$ and c_2 varies from -1 to -2, the system behaves like an underdamped system and the frequency of oscillation of the lateral deviation around its equilibrium point remains constant, but the speed of diminishing its envelope to zero increases by decreasing c_2. For the values of c_2 smaller than -5, the system behaves like overdamped and critically damped systems. If c_1 is increased to -1, the settling time of the overdamped and critically damped responses is increased, as depicted in Fig. 9b.

D. ROBUSTNESS WITH RESPECT TO VEHICLE PARAMETER UNCERTAINTIES

To show the robustness of the proposed algorithm, it is tested in the presence of both disturbance and uncertainties. It is assumed that the nominal values of longitudinal velocity and cornering stiffness parameters are $v_x = 20\frac{\mathrm{m}}{\mathrm{s}}$, $C_f = 170550\ \frac{\mathrm{N}}{\mathrm{rad}}$ and $C_r = 137844\ \frac{\mathrm{N}}{\mathrm{rad}}$, respectively. The disturbance decoupler and tracking controllers are designed with these nominal values, and afterward, random uncertainties of about 20% and 40% of nominal values of the longitudinal velocity and the cornering stiffness parameters are considered in the dynamics, respectively. In addition, it is assumed that disturbances $\omega_1 = \exp(-2t)\cos(4000t)$ and $\omega_2 = \exp(-4t)\sin(6000t)$ are also present. The error states are depicted in Fig. 10. As can be seen, in the presence of both disturbances and the mentioned uncertainties, the output has small variations with respect to the original disturbances, and

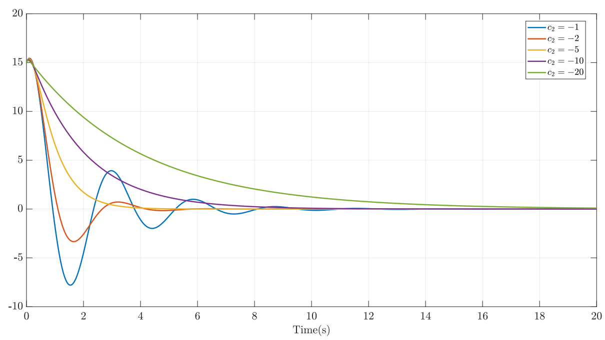

(a) $c_1 = -5$.

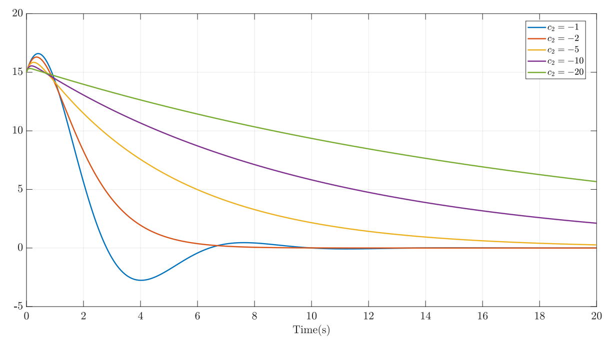

(b) $c_1 = -1$.

FIGURE 9. The effect of changing c_2 on the lateral deviation.

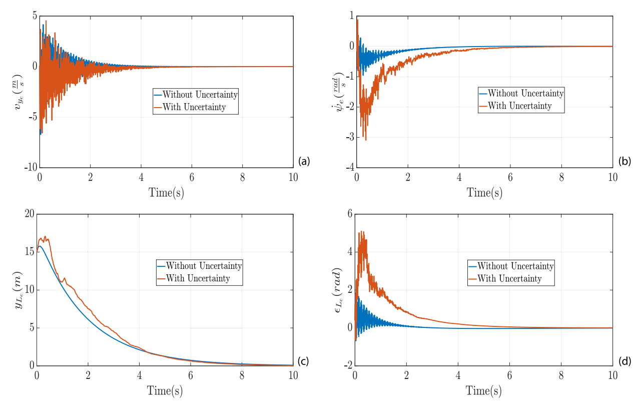

FIGURE 10. Robustness of the proposed method in the presence of both disturbance and uncertainties.

moreover, after attenuation of the disturbances, the tracking part handles the uncertainties and steers the errors to zero.

V. CONCLUSION

In this paper, the nonlinear lateral dynamics of an autonomous vehicle augmented by the lane keeping dynamics were considered. Using a geometric approach, all classes of decouplable disturbances from lateral deviation were obtained and a disturbance decoupling controller was proffered via control invariant property. Afterward, a tracking controller was designed for the augmented nonlinear lateral vehicle dynamics and lane keeping ones by using a controller with a predefined structure. The obtained control law was applied to a typical vehicle in the presence of different disturbances, uniformly distributed and exponentially attenuated, to show the performance and effectiveness of the obtained control law. Moreover, the effect of changing the coefficients of the tracking controller, and the presence of uncertainty in the vehicle parameters were explored in the simulations.

ACKNOWLEDGEMENT

This work was supported in part by the Ministry of Science and Technology (MOST), Taiwan, under Grant MOST.

REFERENCES

[1] S. Liu, L. Li, J. Tang, S. Wu, and J.-L. Gaudiot, *Creating Autonomous Vehicle Systems*. San Rafael, CA, USA: Morgan & Claypool, 2018.

[2] J. Kim, J.-H. Park, and K.-Y. Jhang, "Decoupled longitudinal and lateral vehicle control based autonomous lane change system adaptable to driving surroundings," *IEEE Access*, vol. 9, pp. 4315–4334, 2021.

[3] A. Amodio, M. Ermidoro, S. M. Savaresi, and F. Previdi, "Automatic vehicle model recognition and lateral position estimation based on magnetic sensors," *IEEE Trans. Intell. Transport. Syst.*, early access, Mar. 4, 2020, doi: 10.1109/TITS.2020.2974808.

[4] Y. Huang and Y. Chen, "Vehicle lateral stability control based on shiftable stability regions and dynamic margins," *IEEE Trans. Veh. Technol.*, vol. 69, no. 12, pp. 14727–14738, Dec. 2020.

[5] S. Dixit, U. Montanaro, M. Dianati, A. Mouzakitis, and S. Fallah, "Integral MRAC with bounded switching gain for vehicle lateral tracking," *IEEE Trans. Control Syst. Technol.*, early access, Oct. 1, 2020, doi: 10.1109/TCST.2020.3024586.

[6] M. Liu, K. Chour, S. Rathinam, and S. Darbha, "Lateral control of an autonomous and connected vehicle with limited preview information," *IEEE Trans. Intell. Vehicles*, early access, Oct. 26, 2020, doi: 10.1109/TIV.2020.3033773.

[7] M. Canale, L. Fagiano, A. Ferrara, and C. Vecchio, "Comparing internal model control and sliding-mode approaches for vehicle yaw control," *IEEE Trans. Intell. Transport. Syst.*, vol. 10, no. 1, pp. 31–41, Mar. 2009.

[8] S. Ding, L. Liu, and W. X. Zheng, "Sliding mode direct yaw-moment control design for in-wheel electric vehicles," *IEEE Trans. Ind. Electron.*, vol. 64, no. 8, pp. 6752–6762, Aug. 2017.

[9] A. Ferrara, G. P. Incremona, and E. Regolin, "Optimization-based adaptive sliding mode control with application to vehicle dynamics control," *Int. J. Robust Nonlinear Control*, vol. 29, no. 3, pp. 550–564, Feb. 2019.

[10] R. Wang, H. Jing, C. Hu, M. Chadli, and F. Yan, "Robust H_∞ output-feedback yaw control for in-wheel motor driven electric vehicles with differential steering," *Neurocomputing*, vol. 173, no. 3, pp. 676–684, 2016.

[11] C. Li, H. Jing, R. Wang, and N. Chen, "Vehicle lateral motion regulation under unreliable communication links based on robust H_∞ output-feedback control schema," *Mech. Syst. Signal Process.*, vol. 104, pp. 171–187, May 2018.

[12] X. Wang, M. Fu, H. Ma, and Y. Yang, "Lateral control of autonomous vehicles based on fuzzy logic," *Control Eng. Pract.*, vol. 34, pp. 1–17, Jan. 2015.

[13] J. Guo, Y. Luo, K. Li, and Y. Dai, "Coordinated path-following and direct yaw-moment control of autonomous electric vehicles with sideslip angle estimation," *Mech. Syst. Signal Process.*, vol. 105, pp. 183–199, May 2018.

[14] D. Rubin and S. A. Arogeti, "Vehicle yaw stability control using active limited-slip differential via model predictive control methods," *Vehicle Syst. Dyn.*, vol. 53, no. 9, pp. 1315–1330, Sep. 2015.

[15] J. Zhang, W. Sun, and Z. Feng, "Vehicle yaw stability control via H_∞ gain scheduling," *Mech. Syst. Signal Process.*, vol. 106, pp. 62–75, Jun. 2018.

[16] H. Zhang and J. Wang, "Vehicle lateral dynamics control through AFS/DYC and robust gain-scheduling approach," *IEEE Trans. Veh. Technol.*, vol. 65, no. 1, pp. 489–494, Jan. 2016.

[17] Z. Wang, U. Montanaro, S. Fallah, A. Sorniotti, and B. Lenzo, "A gain scheduled robust linear quadratic regulator for vehicle direct yaw moment control," *Mechatronics*, vol. 51, pp. 31–45, May 2018.

[18] X. Ji, X. He, C. Lv, Y. Liu, and J. Wu, "Adaptive-neural-network-based robust lateral motion control for autonomous vehicle at driving limits," *Control Eng. Pract.*, vol. 76, pp. 41–53, Jul. 2018.

[19] Y. Jia, "Robust control with decoupling performance for steering and traction of 4WS vehicles under velocity-varying motion," *IEEE Trans. Control Syst. Technol.*, vol. 8, no. 3, pp. 554–569, May 2000.

[20] H. Du, N. Zhang, and G. Dong, "Stabilizing vehicle lateral dynamics with considerations of parameter uncertainties and control saturation through robust yaw control," *IEEE Trans. Veh. Technol.*, vol. 59, no. 5, pp. 2593–2597, 2010.

[21] S. Brennan and A. Alleyne, "Dimensionless robust control with application to vehicles," *IEEE Trans. Control Syst. Technol.*, vol. 13, no. 4, pp. 624–630, Jul. 2005.

[22] H. Zhang, X. Zhang, and J. Wang, "Robust gain-scheduling energy-to-peak control of vehicle lateral dynamics stabilisation," *Vehicle Syst. Dyn.*, vol. 52, no. 3, pp. 309–340, Mar. 2014.

[23] A. El Hajjaji, M. Chadli, M. Oudghiri, and O. Pages, "Observer-based robust fuzzy control for vehicle lateral dynamics," in *Proc. Amer. Control Conf.*, 2006, p. 6.

[24] A. M. Perdon and M. Anderlucci, "Disturbance decoupling problem for a class of descriptor systems with delay via systems over rings," *IMA J. Math. Control Inf.*, vol. 27, no. 4, pp. 405–418, 2010.

[25] L. Zhang, J.-E. Feng, X. Feng, and J. Yao, "Further results on disturbance decoupling of mix-valued logical networks," *IEEE Trans. Autom. Control*, vol. 59, no. 6, pp. 1630–1634, Jun. 2014.

[26] E. Zattoni, A. M. Perdon, and G. Conte, "Disturbance decoupling with closed-loop modes stability in switched linear systems," *IEEE Trans. Autom. Control*, vol. 61, no. 10, pp. 3115–3121, Oct. 2016.

[27] B. Li, Y. Liu, K. I. Kou, and L. Yu, "Event-triggered control for the disturbance decoupling problem of Boolean control networks," *IEEE Trans. Cybern.*, vol. 48, no. 9, pp. 2764–2769, Sep. 2018.

[28] J.-K. Seok and S.-K. Kim, "VCM controller design with enhanced disturbance decoupling for precise automated manufacturing processes," *Electr. Power Appl., IET*, vol. 6, no. 8, pp. 575–582, Sep. 2012.

[29] T. R. Grochmal and A. F. Lynch, "Precision tracking of a rotating shaft with magnetic bearings by nonlinear decoupled disturbance observers," *IEEE Trans. Control Syst. Technol.*, vol. 15, no. 6, pp. 1112–1121, Nov. 2007.

[30] J. Lunze and T. Steffen, "Control reconfiguration after actuator failures using disturbance decoupling methods," *IEEE Trans. Autom. Control*, vol. 51, no. 10, pp. 1590–1601, Oct. 2006.

[31] Q. Meng, Z.-Y. Sun, Y. Shu, and T. Liu, "Lateral motion stability control of electric vehicle via sampled-data state feedback by almost disturbance decoupling," *Int. J. Control*, vol. 92, no. 4, pp. 734–744, Apr. 2019.

[32] P. Dugoff and L. Segel, "An analysis of tire traction properties and their influence on vehicle dynamic performance," *SAE Trans.*, vol. 79, pp. 1219–1243, Jan. 1970.

[33] H. Pacejka, *Tire and Vehicle Dynamics*. Oxford, U.K.: Butterworth-Heinemann, 2012.

[34] R. Rajamani, *Vehicle Dynamics and Control*. New York, NY, USA: Springer, 2012.

[35] Z. Chu, Y. Sun, C. Wu, and N. Sepehri, "Active disturbance rejection control applied to automated steering for lane keeping in autonomous vehicles," *Control Eng. Pract.*, vol. 74, pp. 13–21, May 2018.

[36] A. Isidori, *Nonlinear Control Systems*. London, U.K.: Springer-Verlag, 1995.

[37] A. Isidori, A. Krener, C. Gori-Giorgi, and S. Monaco, "Nonlinear decoupling via feedback: A differential geometric approach," *IEEE Trans. Autom. Control*, vol. AC-26, no. 2, pp. 331–345, Apr. 1981.

[38] H. K. Khalil and J. W. Grizzle, *Nonlinear System*, vol. 3. Upper Saddle River, NJ, USA: Prentice-Hall, 1996.

[39] G. Tagne, R. Talj, and A. Charara, "Design and comparison of robust nonlinear controllers for the lateral dynamics of intelligent vehicles," *IEEE Trans. Intell. Transp. Syst.*, vol. 17, no. 3, pp. 796–809, Mar. 2016.

MOHAMMAD REZA SATOURI was born in Bushehr, Iran, in 1992. He received the B.Sc. degree in telecommunications from Persian Gulf University, Bushehr, and the M.Sc. degree in control systems from the University of Tehran, Tehran, Iran. He was with the Smart Networks Laboratory, University of Tehran. He is currently a Researcher with the Dynamical Systems and Control (DSC) Research Laboratory, Persian Gulf University. His research interests include optimal control systems, game theory, autonomous vehicles, adaptive dynamic programming, and reinforcement learning.

ABOLHASSAN RAZMINIA was born in Bushehr, Iran, in 1982. He received the B.Sc. degree in control systems from Shiraz University, Shiraz, Iran, in 2004, the M.Sc. degree in control systems from the Shahrood University of Technology, Shahrood, Iran, in 2007, and the Ph.D. degree in control systems from Tarbiat Modares University, Tehran, Iran, in 2012. He is currently an Associate Professor with the Department of Electrical Engineering, School of Engineering, Persian Gulf University, Bushehr. His research interests include optimal control systems, nonlinear dynamical systems, and system identification.

SALEH MOBAYEN received the B.Sc. and M.Sc. degrees in control engineering from the University of Tabriz, Tabriz, Iran, in 2007 and 2009, respectively, and the Ph.D. degree in control engineering from Tarbiat Modares University, Tehran, Iran, in January 2013. From February 2013 to December 2018, he was an Assistant Professor and a Faculty Member with the Department of Electrical Engineering of University of Zanjan, Zanjan, Iran. Since December 2018, he has been an Associate Professor of control engineering with the Department of Electrical Engineering, University of Zanjan. He currently collaborates as an Associate Professor with the Future Technology Research Center, National Yunlin University of Science and Technology. He has published several articles in the national and international journals. His research interests include control theory, sliding mode control, robust tracking, non-holonomic robots, and chaotic systems. He is a member of the IEEE Control Systems Society and serves as a member of program committee of several international conferences. He is an Associate Editor of *Artificial Intelligence Review*, the *International Journal of Control, Automation and Systems*, *Circuits, Systems, and Signal Processing*, *Simulation*, *Measurement and Control*, the *International Journal of Dynamics and Control*, and *SN Applied Sciences*. He is an Academic Editor of *Complexity*, *Mathematical Problems in Engineering*, and other international journals.

PAWEŁ SKRUCH (Senior Member, IEEE) received the M.S. degree (Hons.) in automation control from the Faculty of Electrical Engineering, Automatics, Computer Science and Electronics, AGH University of Science and Technology, Krakow, Poland, in 2001, the Ph.D. degree *(summa cum laude)* from the AGH University of Science and Technology, in 2005, and the D.Sc. (Habilitation) degree in automatics and robotics from AGH University, in 2016. He is currently a Professor of control engineering with the AGH University of Science and Technology, and an Advanced Engineering Manager AI & Safety with the Aptiv Technical Center, Krakow. His current research interests include dynamical systems, autonomous systems, artificial intelligence, machine learning, modeling and simulation, and applications of control theory to software systems.